Chapter 6
Multi-Scale Energy Harvesting

Weisi Guo, Yansha Deng, Arumugam Nallanathan, Bin Li, and Chenglin Zhao

6.1 Introduction

One of the key trends over the past half a century has been that technology is getting smaller, faster, cheaper, and more powerful every day. In terms of computing technology, the key components have become 100-times smaller each decade. For example, the ENIAC computer (1956) used to fill a warehouse, and its equivalent compute power now sits inside a musical greeting card at the price of $4. Standard smartphones today have more computing power than the personal computers (PCs) of a decade ago. Today, this miniaturization trend continues in the form of personal wearables that can perform many of the functions of smartphones and pads of yesteryear. Smaller devices not only enable a greater number of them in any given space, but also enable mobility and personalization. It is envisaged that device miniaturization will lead to over 50 billion devices connected to the Internet, forming a large part of the Internet-of-Things (IoT) paradigm. The consequence is that devices are getting closer to the human body and integrating and interacting with our lifestyles. Inevitably, as device dimensions reduce to microns, they are able to be inserted inside our body to achieve precision sensing, communications, and actuation; potentially transforming health-care. In fact, the Internet of Nano Things (IoNTs) has been named as one of the top ten emerging technologies by the World Economic Forum in 2016.

W. Guo (✉)
University of Warwick, Coventry, UK
e-mail: weisi.guo@warwick.ac.uk

Y. Deng • A. Nallanathan
Kings College London, London, UK

B. Li • C. Zhao
Beijing University of Posts and Telecommunications (BUPT), Beijing Shi, China

D.N.K. Jayakody et al. (eds.), *Wireless Information and Power Transfer: A New Paradigm for Green Communications*, DOI 10.1007/978-3-319-56669-6_6

The energy efficiency of systems in general determines its operational sustainability. For small devices, removing the power-tether is an important mobility enabler. Such devices today include sensor motes, radio frequency (RF) tags, and wearable computers. When there is limited recharging or energy storage capability, ad-hoc harvesting of energy is a crucial technology for a variety of systems. These devices need to harvest energy from alternative sources such as natural environment or even intercepting ambient wireless signals. Energy harvesting techniques not only prolong operational life-time of such devices and reduce their infrastructure dependency, but also allow devices to be deployed in any location deemed desirable and be mobile. Harvesting energy from high frequency electromagnetic radiation (i.e., visible band) has been most widely used in photovoltaic cells, but requires direct sunlight which may not always be readily available when devices are embedded inside or in the shadow of objects. Consequently, energy harvesting from low frequency information transmissions (i.e., radio band) have been proposed as an alternative.

A variety of wireless systems and devices that transmit across multiple distance scales fit this profile, from relatively power-hungry macro-base stations (BSs) deployed in remote regions, to nano-scale sensors in vivo environments (i.e., embedded sensors that monitor wound healing status). The wide range of devices transverse multiple device length scales and communicate across distance scales that vary by up to 9 orders of magnitude (from km to microns). Yet, it remains unclear what set of energy harvesting technologies are suitable for the different dimension and distance scales, as well as diverse operating environments. RF energy harvesting solutions have recently been proposed as an alternative [1], especially for low-power devices such as sensor motes in urban and semi-urban environments [2, 3]. The concept has been around since the 1970s [4]. For example, it has been shown experimentally that the power delivered at a location that is 20 km away from a 150 kW TV transmitter or within 30 m from a cellular BS [5] is typically in the order of 0.1 mW [6, 7]. Recent advances in this area have shown that energy - efficient transmitters can be entirely powered by RF energy harvesting devices, which use cognitive methods to sense fruitful primary-network spectrum bands for targeted energy harvesting [8] or sensing traffic patterns for targeted deployment of nodes [9], and simultaneous wireless information and power transfer is possible (SWIPT) [10, 11]. Given knowledge of the location of a RF energy source, a receive antenna array can be appropriately configured to further improve energy harvesting efficiency. However, little is known about the peak power or reliable energy level that can be harvested from multiple transmitters of different radio networks (e.g., cellular base stations, Wi-Fi access points, and mobile handsets).

This chapter will review state-of-the-art technologies that allow multi-scale wireless devices to simultaneous harvest energy and transmit data, especially from a number of different wireless signal sources. The chapter will be organized into different technology dimension scales, and focus on both the fundamental scientific principles and opportunities and the engineering challenges. The key sections are listed as follows:

1. Macro-/Meso-scale energy harvesting for small devices such as RFID tags. The focus will be on the potential of crowd harvesting from multiple radio transmissions in complex urban environments.
2. Micro-/Nano-scale energy harvesting for nano devices such as drug delivery robots and embedded health monitoring devices. The focus will be on information and energy bearing bio-molecules and drawing inspiration from equivalent biological processes.

We now present the detailed outline of each of the aforementioned sections.

6.2 Macro-/Meso-Scale Energy Harvesting

Current cellular and long-distance wireless systems are relatively large in dimension and consume significant power (i.e., each antenna element can consume up to 600 W [12]). There are already efforts to reduce the power consumption of wireless infrastructures such as macro-/metro-BSs. In certain rural areas that lack reliable and sufficient electricity coverage, energy harvesting from solar radiation is possible [13]. Certainly this is an active area of research for cellular network vendors such as Alcatel-Lucent. The challenge lies in optimizing data transmission and sleep mode in the face of an unreliable energy source with the aid of energy storage [14]. On a smaller scale, femto-BSs and other small-cell technologies (i.e., wireless relays), which are often deployed in areas that require coverage compensation and may not have access to electricity in the immediate vicinity, are likely to demand 10–100 W of power. As such, indoor optical wireless systems have been proposed to transfer power to small cells at night time [15]. Nonetheless, it remains challenging to power a large wireless system using entirely energy harvesting. Several realistic problems related to obstacles that obstruct the energy beams and unexpected high traffic demand can lead to unacceptable levels of service outage.

Smaller meso-scale systems are likely to demand a significantly lower level of power, varying from 1 mW to 1 W. As such, harvesting energy from wireless transmissions becomes possible. This section will examine the potential of crowd harvesting energy from all neighbouring transmissions with particular emphasis on large-scale network modeling and theoretical bounds under full and variable traffic patterns.

6.2.1 Crowd Energy Harvesting

6.2.1.1 Background

Over the past decade, increased urbanization and growing demands for wireless data have led to a dramatic increase in the number and density of wireless transmitters in

cities. The global cellular infrastructures constituted more than four million macro-BSs and served more than seven billion active user equipments (UEs) in 2013. Moreover, public and privately owned Wi-Fi access points (APs) in developed cities have reached the density of over 350/km^2, with top metropolitan cities reaching over 700/km^2. With IoT devices equipped with wireless capabilities, it is expected the number of wireless devices will exceed 50 billion by 2020.

Despite the growing density of RF transmitters in urban areas, doubts remain with regard to the amount of RF energy that they can provide over a period of time. Whilst the increase in transmitter density will undoubtedly increase the amount of RF energy available in urban environments, a few challenges in large-scale reliable RF energy harvesting are undeniable. As shown in Fig. 6.1, some of these challenges are: (1) the random nature of RF transmitter locations, (2) stochastic elements in the RF propagation channel, and (3) variations in spectrum utilization due to varying data traffic patterns (i.e., sensors may only transmit data occasionally), all of which need to be carefully considered in the design of an efficient RF energy harvesting system. For example, the fluctuating harvested energy due to channel

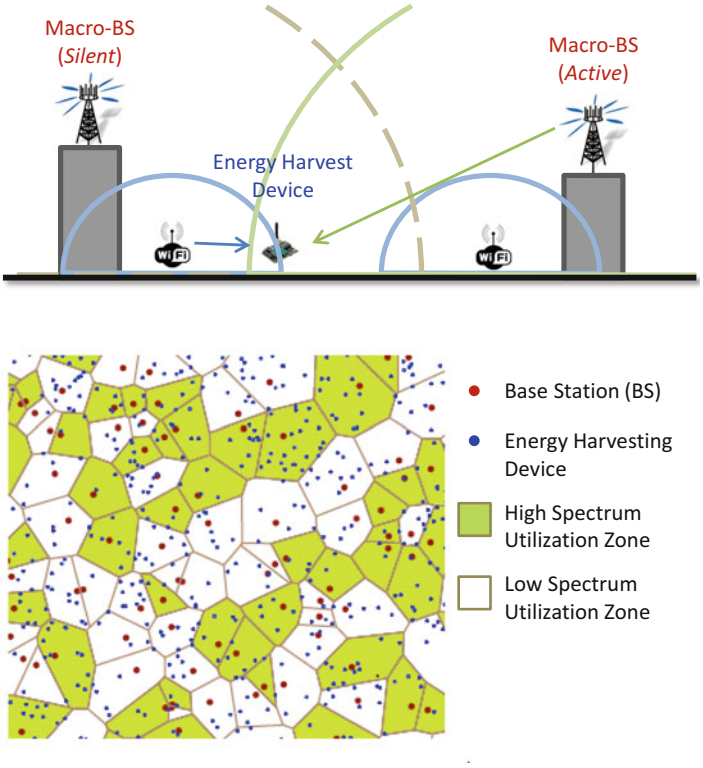

Fig. 6.1 Illustration of large-scale RF energy harvesting by multiple RF transmitters. On any particular spectrum band, the transmitter may or may not be transmitting, depending on the local traffic load

fading and node movements needs to be converted into constant DC voltage using a capacitor. However, longer-term stable energy harvesting is harder to predict and more difficult to compensate for. Understanding the long-term energy harvesting reliability is important for energy aware transmission protocols and for devices that have a limited battery capacity [16].

6.2.1.2 Hardware

Energy harvesting of electromagnetic radiation is most widely used by photovoltaic cells. However, direct sunlight is not always readily available. RF harvesting solutions have been proposed as an alternative [6, 17, 18]. By amalgamating multiple radio signals, RF energy harvesting has the greatest potential in urban areas, where there is an abundance of wireless communication devices from multiple Radio-Access-Technologies (RATs). Due to stochastic signal strength variations, the fluctuating harvested power can be converted into constant DC voltage using a capacitor. Recently, it has been shown that the power delivered is typically in the order of 0.1 mW at a location that is 20 km away from a 150 kW TV transmitter [7], or within a short range of 30 m from a cellular BS [5]. Several commercial devices exist with reasonably low sensitivity (i.e., −11 dBm of the P2110 Powerharvester) and significantly higher sensitivities are needed to harvest from a wider variety of RF signals. Even with improved energy harvesting circuits, little is known about the power lever that can be delivered in RF bands other than the TV channels and when devices attempt to harvest from the increasingly densely deployed BSs, Wi-Fi hotspots, and even mobile handsets. Due to stochastic variations in RF signal strength and traffic load (for example, BS traffic is notoriously stochastic [19]), the harvested power level fluctuates over time and needs to be converted into constant DC voltage using a capacitor. However, long-term stability is harder to predict and more difficult to compensate for. Existing performance tests have focused on specific scenarios: *single dominant link* (e.g., transmission from a nearby TV-station) [6], or field tests in a small experimental area, typically without considering the effects of: *multi-path*, *shadowing*, *traffic load*, and *mobility* [20].

6.2.1.3 Modeling Crowd Energy Harvesting Potential

Considering energy harvesting from a large number of fixed RF transmitters, it is possible to calculate the specific pathloss for each channel and predict the energy harvesting performance. The computational complexity grows linearly with the number of energy harvesting devices. If there is a lack of perfect knowledge of transmitters' locations, e.g., private Wi-Fi APs and mobile phones, predicting the energy harvesting performance becomes impractical if not impossible. Therefore, an accurate statistical notion of the available ambient RF energy as a function of the wireless networks interested and the associated propagation environment is needed. Stochastic geometry studies random spatial patterns, formed by spatial point

processes. The underlying principle is that the locations of network transmitters are random in nature, but their density and mutual distances follow certain statistical distributions. This knowledge can be used to create tractable statistical frameworks for analysing the performance of wireless networks [21]. In order for the results to be accurate, the spatial distribution of the network nodes must be derived from empirical cell location data. In this section, we offer a review of the spatial distributions of cellular macro-BSs and present new data and spatial distributions for femto-BSs and Wi-Fi APs.

In order to estimate the energy received from a large number of RF transmitters, one needs to know the probability distribution of the distance between the kth nearest RF transmitter and the energy harvesting device. In the literature, two independent sets of macro-BS data and mathematical proofs have produced the same spatial distribution of macro-BSs [22, 23]. The probability density function (pdf) of the distance r between the energy harvesting device at an arbitrary location and the kth nearest macro-BS is given by

$$f_{\mathrm{BS},R_k}(r;k) = \frac{2(\Lambda\pi)^k}{(k-1)!} r^{2k-1} e^{-\Lambda\pi r^2}, \quad k \geqslant 1, \tag{6.1}$$

where Λ is the average spatial density of macro-BSs in an area where the signal power is high enough to be considered. Such an area is approximately $4\,\mathrm{km}^2$ for urban environments concerning macro-BSs. The $k = 1$ case (i.e., the nearest macro-BS), which follows a Rayleigh distribution, is most commonly considered in wireless communications.

In recent years, femto-BSs are being deployed with increasing densities in urban areas. Empirical data obtained has shown that the spatial distribution of the kth nearest femto-BS is identical to that of macro-BSs. That is to say, despite the tedious multi-variable optimization for cellular network planning, macro- and femto-BSs are in fact randomly deployed with the spatial distribution of the kth nearest BS given by (6.1). In the literature, Poisson cluster processes (PCPs) such as the Matern and Thomas cluster processes have been utilized for modeling ad-hoc and small-cell networks [24], but there is a lack of evidence base for such PCP-based modeling.

Wi-Fi APs are deployed in a fundamentally different way to cellular BSs. Their higher density,[1] possibly different spatial distribution, and higher traffic load may yield a different prospect in terms of energy harvesting. Note that the vast majority of Wi-Fi APs are owned by private residential or individual business entities, as opposed to network operators, and both the density and number of Wi-Fi APs change over time. Therefore, the locations of Wi-Fi APs are not exactly known. Whilst certain efforts have been made to locate Wi-Fi APs using directional spectrum sensing approaches [25], a more systematic approach is to infer Wi-Fi APs' locations and density through residential and business census data.

[1] In urban areas, the deployment density of Wi-Fi APs has grown over the past decade to 400–1000 APs per square km.

By assigning a Wi-Fi AP to each residential or business registration address, one can infer the approximate locations of Wi-Fi APs. Based on this data, two discoveries were made [11]: (1) the density distribution of Wi-Fi APs is a log-normal distributed cluster process, commonly found in the ions of materials [26], and that (2) the pdf of the distance between a random point in space and the kth nearest Wi-Fi AP follows the Gamma distribution, i.e., $f_{\text{Wi}-\text{Fi},R_k}(r;k) \sim \Gamma(k,\theta)$, where θ is the scale parameter. What remains undiscovered is the precise distribution of Wi-Fi APs in terms of the scale parameter θ, and the precise spatial distribution of mobile UEs.

6.2.1.4 Full Spectrum Utilization Upper-Bound Analysis

In this section, we consider the aggregated RF power density (Watts per Hz) over a bandwidth of B and from an area with an average transmitter density of Λ. We first assume that all transmitters are transmitting across the whole spectrum available and emit with the maximum allowable power spectrum density on all frequency bands, and hence this is an upper-bound analysis. Leveraging the spatial distributions of RF transmitters found in the previous section, the total *average received RF power* from K RF transmitters is given by

$$P^*_{\text{rx}}(\alpha,\lambda) = B\sum_{k=1}^{K}\int_0^{+\infty} P_{\text{tx}}\lambda r_k^{-\alpha} f_{R_k}(r_k;k)\,\mathrm{d}r_k, \tag{6.2}$$

where P_{tx} is the transmit power, λ is the frequency dependent pathloss constant, α is the pathloss distance exponent, and $f_{R_k}(r_k;k)$ is given in (6.1).

As an example, let us consider the aggregate harvested power P_{rx} for a deployment of macro-BSs that follow the spatial distribution given by (6.1). By integrating (6.2), the total power harvested is found to have the following scaling relationships:

- Linearly proportional to the transmit power: $P^*_{\text{rx}} \propto P_{\text{tx}}$;
- Exponentially proportional to the cell density: $P^*_{\text{rx}} \propto (\Lambda)^{1+\frac{\alpha}{2}}$.

Alternative spatial distributions of RF transmitters are likely to yield different solutions.

A key question at this stage of the analysis is: given that transmitters further away are unlikely to contribute much more power, what is the power difference between harvesting from only the closest transmitter and crowd harvesting? Based on both simulation and the analytical expression in (6.2), the latter can harvest approximately 5–10% more power than the former. Note that this considers only *power*. When *energy* is considered, one also needs to take into account spectrum utilization over time. The reliability of crowd harvesting energy over time will improve dramatically over targeting just a single transmitter.

6.2.1.5 Variable Spectrum Utilization Analysis

In the previous section we have studied the upper-bound to the amount of power that can be harvested from a number of RF transmitters. In order to estimate the harvestable RF energy, it is important to consider the spectrum utilization over time for each RF transmitter. Spectrum utilization depends on the traffic load of each transmitter. Unlike TV channels, which are fewer in number and broadcast over long periods, cellular and Wi-Fi network nodes transmit on demand and the demands can fluctuate in unpredictable temporal and spatial patterns.

Over the past decade, wireless network traffic has shifted from mainly circuit-switched call traffic to packet-switched data traffic dominated. Whilst voice call traffic is well understood, data traffic arrival and departure patterns are much more diversified and unpredictable over time and geographical locations. In this subsection, we leverage the statistical attributes of real 3G HSPA data from a European city's 3G network [27]. Two key observations have been made in all cellular network areas used for traffic data collection:

1. The mean traffic R_k at the kth BS is related to the mean capacity of the BS. In other words, given that each BS has the same bandwidth, cells having superior propagation conditions emit greater energy. The relationship between the traffic and the BS capacity C_k is approximately logarithmic, i.e., $R_k \sim \log_{10} C_k$ [27].
2. The pdf of the traffic load L_k at the kth BS is exponentially distributed, i.e., $f_{L_k} \sim \exp(\tau)$, whereby the rate of decay τ is the same for each cell and varies slowly with time (e.g., hours in a day, and days in a week) [19].

Given knowledge of the statistical properties of data traffic, one can infer the spectrum utilization pattern at each BS as a ratio of the traffic and the peak capacity of the BS, i.e., $L_k = \frac{R_k}{C_k}$. Given that each of the K BSs is independent and identically distributed in space and in spectrum utilization, the pdf of the power density (Watts per Hz) harvested from the sum of all K RF transmitters is the K-fold continuous convolution of the traffic load pdf and the inverse of the received power upper-bound from (6.2):

$$f_{P_{\text{rx}}} = \bigotimes_{k=1}^{K} f_{L_k} / P^*_{\text{rx}}. \tag{6.3}$$

The cumulative distribution function (CDF) of harvested power density (Watts per Hz) shows the reliability of harvestable power density at any given instance in time, where the main variation is derived from the spectrum utilization pattern. By aggregating the CDF over both the frequency bands and time, we can obtain the total expected RF energy that is harvestable.

6.2.2 Case Study: Central London

6.2.2.1 Above Ground

In this section, we consider a central London case study area detailed in [28] that is of 9 km wide and 5 km long. It covers Hyde Park, parts of the Thames River, and major tourism hotspots such as Trafalgar Square, Piccadilly Circus, the Parliament, China Town, London Eye, and Oxford Street. Multiple RATs are included: (1) 4G Cellular Macro-BS Downlink (50 MHz); (2) 4G Cellular UE Uplink (20 MHz); (3) Wi-Fi AP Downlink (20 MHz); and (4) TV Broadcast (100 MHz). The main parameters of the case study are given in Table 6.1.

Table 6.2 shows the mean peak power for different RATs on the per 20 MHz band level, with the whole spectrum available to each RAT. This was a study conducted in [28]. It can be seen that the greatest opportunity for power harvesting lies in the Wi-Fi and TV broadcast RATs. In fact, given that the network traffic on Wi-Fi and TV is typically higher than that of the cellular RAT, it is advisable to focus energy harvesting in these bands, at least before femto-BSs are more widely deployed. By comparing with existing test observations that 100 μW can be achieved at a 20 km distance from a 150 kW TV station [7] or within 30 m from a cellular BS [5], we can see that in general the mean energy harvestable is approximately 5–10 times lower than the special cases tested in [5, 7]. This is primarily due to the log-normal shadow fading considered in our model, as well as the non-line-of-sight (NLOS) positioning of the energy harvesting devices with respect to the RF transmitters.

Due to the small number and fixed locations of TV masts, their energy harvesting potential has been well analysed. We now focus on the effect of Wi-Fi APs' density, number of spectrum bands, and the shadow fading variance on the power harvesting effectiveness. Figure 6.2 shows the simulated aggregate power available to harvest for various Wi-Fi hotspot densities and number of bands available (each band having a bandwidth of 20 MHz). In the simulations, a number of cellular and TV bands are also in operation, with static parameter values set to the peak values shown in Table 6.1. The simulation results show that for a high Wi-Fi density (1000/km^2), the ambient RF power available is in the order of μW, depending on the number of spectrum bands.

Figure 6.3 shows the simulated aggregate power available to harvest versus various Wi-Fi hotspot densities and log-normal shadow fading variance. We can see that when log-normal shadow fading is considered, the average RF power available for harvesting degrades log-linearly with the shadowing variance. In realistic channel conditions, the shadow fading variance can be up to $\sigma^2 = 9$ dB [29]. Compared to the case with no shadow fading, the RF power available for harvesting is lowered by 9 dB for the 3 dB shadow fading variance, and 35 dB for the 6 dB shadow fading variance. *Accordingly, in order to achieve a good RF energy harvesting performance, the devices need to be deployed at locations that experience a shadow fading variance of no greater than 3 dB.*

Table 6.1 London simulation case study parameters

Parameters	Symbol and value
Case study environment	
Geographic area	Central London, 45 km^2
Energy harvester location	Uniform random
No. of energy harvesters	500
Duration of study	2 week period
Propagation model	3GPP urban micro [29]
Pathloss constant	λ, 10^{-4}
Pathloss distance exponent	α, 2–4
Channel fading	Rayleigh
Shadow fading	Log-normal (3 dB variance)
Traffic and spectrum	
Spectrum utilization pdf	f_{L_k}
User arrival pdf	Poisson
Data traffic pdf	Log-normal
Traffic time sample	15 min
4G cellular RAT	
Total no. of macro-BSs	96
Macro-BS density	$\Lambda_{\text{macro}-\text{BS}}$, 2/$km^2$
Macro-BS distribution	Uniform random [22]
Macro-BS transmit power	$P_{\text{tx, macro}-\text{BS}}$, 40 W
Total no. of UE	700,000
UE density	Λ_{UE}, 15,500/km^2
UE distribution	Uniform random (assumed)
UE transmit power	$P_{\text{tx, UE}}$, 0.1 W
Total no. of Wi-Fi APs	45,000
Wi-Fi AP density	$\Lambda_{\text{Wi}-\text{Fi}}$, 1000/$km^2$
Wi-Fi AP distribution	Log-normal cluster based
Wi-Fi AP transmit power	$P_{\text{tx, Wi}-\text{Fi}}$, 1 W
Total no. of TV masts	4–5
TV mast density	Λ_{TV}, 0.1/km^2
TV mast distribution	Fixed
TV mast transmit power	$P_{\text{tx, TV}}$, 1000 kW

As shown previously in (6.3), the energy harvested depends on the convolution between the peak power available for harvesting and the pdf of the spectrum utilization level. The peak power value given by (6.2) is largely determined by the spatial distribution and density of RF transmitters, as well as the propagation environment itself. We have shown that the harvested power value can be improved by 5–10% through crowd harvesting as compared to harvesting from the closest transmitter only. Moreover, the spectrum usage can be dynamic and in the event that the closest transmitter is not transmitting, crowd energy harvesting shines. When

Table 6.2 London case study results with different RATs [28]

RAT	*Peak power per band* (μW/sqm)
Cellular downlink	0.3
UE uplink	1
Wi-Fi downlink	5
TV broadcast	1.2
RAT	*Peak power* (μW/sqm)
Cellular downlink (50 MHz)	0.6
UE uplink (20 MHz)	1
Wi-Fi downlink (20 MHz)	5
TV broadcast (100 MHz)	6
RAT	*Aggregate daily energy*
Cellular downlink (50 MHz)	5 mJ/sqm
UE uplink (20 MHz)	4.2 mJ/sqm
Wi-Fi downlink (20 MHz) 8	0.13 J/sqm
TV broadcast (100 MHz)	0.5 J/sqm

Peak power and aggregate daily energy harvested averaged across all devices over a 2 week period

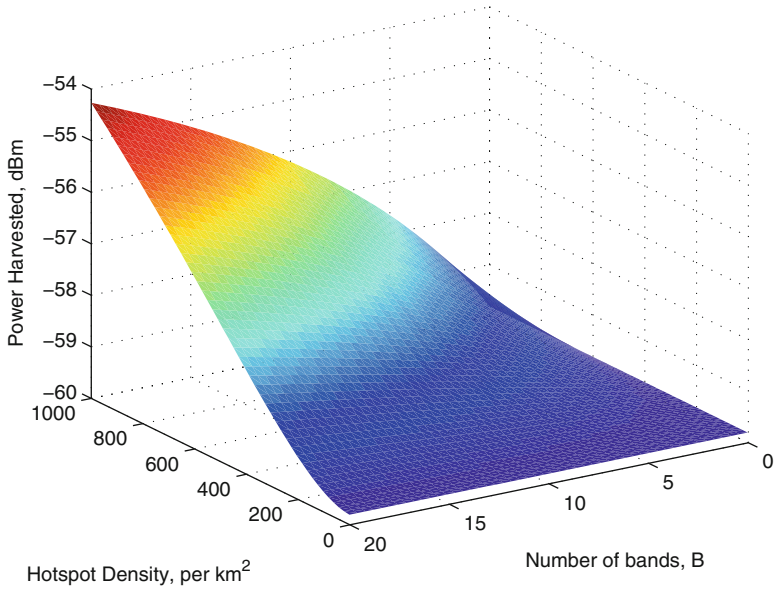

Fig. 6.2 Simulated aggregate power available to harvest for various Wi-Fi hotspot densities and number of bands available

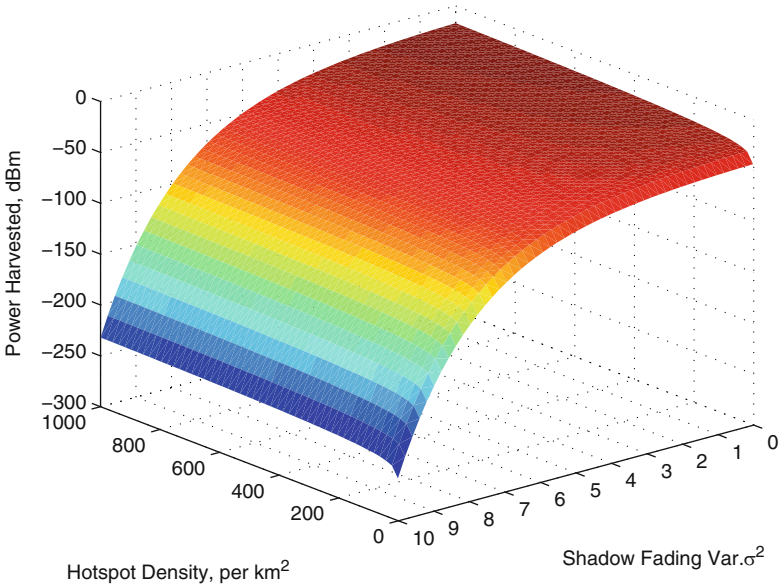

Fig. 6.3 Simulated aggregate power available to harvest for various Wi-Fi hotspot densities and shadow fading variances (dB)

the investigation factors in the variational spectrum utilization, it is apparent that the total energy harvested from all ambient RF transmitters will produce a fixed 5% of improved reliability in energy delivery per second over that from the strongest transmitter. For a fixed reliability demand (i.e., deliver at least a certain power level for at least 30% of the time), the power harvested has improved from 4 μW (harvesting from the closest transmitter only) to 8.5 μW (crowd harvesting), an improvement of over 100%. This is primarily down to exploiting diverse variations in spectrum utilization at different transmitters by harvesting energy from a diverse range of radio sources. The aggregate daily energy harvested (averaged across all devices) is given in Table 6.2. It shows that Wi-Fi and TV broadcast remain the most promising bands to harvest because of their wider bandwidth and greater spectrum utilization due to higher traffic.

6.2.2.2 Below Ground

Table 6.3 shows a different study conducted for central London detailed in [2] for underground stations. The study uses real measurement data across from 400 MHz to 2.5 GHz to test the average and peak received power density. The results show that GSM900 and GSM1800 and 3G all have similar high energy harvesting potential, whilst Wi-Fi and DTV remain significantly weaker (by approximately

Table 6.3 London underground case study results with different RATs [2]

RAT	Average power (μW/sqm)	Peak power
Cellular downlink (75 MHz)	840	64 mW/sqm
UE uplink (75 MHz)	5	200 μW/sqm
Wi-Fi downlink (100 MHz)	1.8	60 μW/sqm
TV broadcast (140 MHz)	8.9	4.6 mW/sqm

Average power density and maximum power density

20 dBm/sqcm). These results seem to indicate that in reality BSs are a far better source of energy harvesting than DTV and Wi-Fi, possibly because of the nature of the embedded underground environment.

6.2.3 Optimization for Crowd Harvesting

We have so far reviewed the potential of crowd harvesting across different RATs, which is attractive, especially in the TV bands (LoS) and Wi-Fi bands (NLoS). However, what remains unclear is how a relay system, where the nodes are sufficiently apart (and hence have different energy harvesting potentials), can collaborate to achieve optimal relaying performance. In this section we discuss node collaboration and transmission scheduling for crowd harvesting [11]. It has been revealed that the correlation distance of the traffic density is less than 80 m in urban areas [30], indicating that the RF energy harvesting process may follow similar spatial correlation. Two nodes that are more than 100 m apart tend to have almost independent energy harvesting processes, and thus node collaboration can be performed to exploit the independent relationship between energy profiles, e.g., to achieve energy harvesting diversity gains.

First we illustrate the benefit of node collaboration via combining the SWIPT and ambient energy harvesting, in order to compensate for the possible energy shortage. Assuming that the source can harvest more ambient RF energy than the relay node, the energy harvesting phase can be split further into two parts: (1) source-to-relay energy delivery, and (2) ambient RF energy harvesting at relay. Note that the source can make use of the time when the relay forwards the message, to harvest additional ambient RF energy. Furthermore, for the scenario where the nodes have no SWIPT structure or have some common information to the same destination, for example, the multiple relays in the second hop of a relaying transmission, or multiple sensors that sense the same target and need to deliver the sensing results to the sink. In this case, collaborative transmission can be used to address the uneven energy arrival rates. As a simple example, a transmission frame can be divided into two subframes. In the first subframe, only one of the nodes can be scheduled to transmit in the conventional way. In the second subframe, multiple nodes can perform simultaneous joint transmission (JT) to the destination with distributed beamforming. To this end,

the frame division portion and the node scheduling should be jointly optimized, taking into account the ESI of all nodes. For both cases, to get the optimal system parameters, practical online algorithms should be designed based on the prediction of the mobile traffic that generates the crowd EH source. One can model the mobile traffic variation with Markovian model, of which the transition probabilities can be trained based on real data [11], and then MDP policy iteration will provide the optimal transmission scheduling and system parameters. To reduce the complexity of MDP, one can do conventional optimization on a per-frame basis, with the energy arrivals and channel conditions of several future frames as known, given the traffic prediction precision is high.

6.2.4 Summary and Discussion

Most existing work on energy harvesting has focused on the hardware design of energy harvesting devices. Field tests of those devices are typically in LoS with a nearby BS or TV mast. Whilst the results are beneficial, they reveal very little about how such devices will perform when mass deployed in an urban environment. In an urban mass deployment, the energy harvesting devices may need to be at locations to serve a purpose (e.g., to sense the pollution level at a specific location) and there is very little flexibility in alternative locations. Such locations are likely to be in NLoS from RF transmitters, and far away from powerful TV mast transmitters. Crowd energy harvesting can leverage the growing density of BSs, Wi-Fi APs, and mobile UEs. However, an analytical framework backed up by empirical data has been absent thus far. This review paper has shown that stochastic geometry has the potential to provide a upper-bound to the power available to harvest (6.2), provided that we know the spatial distribution of the transmitters. Further understanding of the traffic patterns can yield insight into the spectrum usage level. By convolving the upper-bound of the power from multiple transmissions with the spectrum utilization probability function, the reliability distribution of energy harvesting from multiple sources can be found (6.3).

What the preliminary study has shown can be summarized as:

- The upper-bound power available for harvesting scales linearly with transmit power, and exponentially with the transmitter density. This is sensitive to both the pathloss distance exponent and the spatial distribution of the transmitters. Harvesting power from multiple sources offers a 5–10% improvement over harvesting from only the closest source.
- The reliability of the energy available for harvesting depends on the upper-bound power, as well as the traffic pattern. The pdf of the spectrum utilization typically follows a log-normal distribution. Harvesting energy from multiple sources offers greater diversity, which translates into a 5% improvement in reliability and 100% improvement of energy level as compared to harvesting from the closest source.

There remains plenty of further work to be carried out, including large-scale field trials, finding accurate spatial distributions for transmitters of different RATs, as well as their traffic load distributions. Whilst TV and cellular networks are relatively well understood, Wi-Fi and mobile UEs are not. Yet, it is the Wi-Fi APs and mobile UEs that could potentially grow the fastest in terms of transmitter density, and their cluster-like spatial distributions offer the greatest prospect of improving crowd RF energy harvesting.

6.3 Micro-/Nano-Scale Energy Harvesting

6.3.1 Introduction

Today, micro-electronic devices can perform comparable operations to analog electronic machines that used to occupy a factory floor. One consequence of increasing device miniaturization is that we can now carry, wear, and embed advanced machinery on or inside ourselves. As the technology for mobile and wearable devices matures, research focus has now shifted towards embedded devices for health monitoring. Whilst macro-scale implantable devices (i.e., pacemakers) can trace its origin back to late 1950s, a new generation of micro-scale sensors can monitor a variety of physical and biochemical states (i.e., wound recovery, hormone levels) in the human body are being developed.

Nano-machines or nano-robotics define a broad number of devices comprised of components that are close to the scale of a nanometre. Nano-machines have a variety of applications that range from precision drug delivery, real-time sensing, and controlling cell dynamics. Nanotechnology in this context has emerged greatly in the early state (theoretical designs and simulated performance testing, with a few in vitro and in vivo tests), although there are still some limitations for further development. Currently, nano-machines lack the ability to communicate with each other, limiting their potential to perform coordinated tasks. For example, coordinated and controlled (via light, pH, swelling/shrinkage, etc.) drug delivery can maximize the therapeutic range and minimize toxicity and ineffectiveness. Being able to achieve nano-scale communications will herald a new era of nano-medicine: connecting a plethora of nano-sensors and realizing a key component in the Internet of Bio-Nano things (IoBNT) paradigm [31].

IoBNT systems are an essential component of nano-medicine, which promises to revolutionize health-care. The demand for precision medicine such as nano-machines operating in vivo environments is immense (current market valued at $100 billion with a 14% CAGR). One example application area is coordinated drug delivery. Today, poor drug delivery effectiveness costs the world $ billions and exposes patients to the risk of high toxicity. Normal delivery of drugs through the digestion and blood stream causes a long exposure to toxicity across a wide range of cells. In effect, the therapeutic range is small and waste is high.

Coordinated drug deliveries by mechanical and chemically triggered processes are sensitive to the unpredictable in vivo environment, and do not achieve coordination between devices. Coordinated drug delivery by a swarm of nano-machines that can coordinate a simultaneous payload release can improve the therapeutic range and decrease toxicity risk and waste. Wireless communication between such robots and the outside world is necessary for the purposes of command and control, and monitoring. Yet, wireless communication is extraordinarily challenging at the nano-scale in fluidic in vivo environments, i.e., small device dimension limits electromagnetic waves to be at the lossy THz band. On the other hand, cells use molecular signaling. Drawing an inspiration from these processes, researchers have set out to design functional bioengineering sub-systems (i.e., remote controlled DNA-circuits and bacteria systems [32]), as well as molecular communication sub-systems [33]. In converting theoretical designs into practice, recent progress in building macro-scale prototypes [34, 35] has allowed researchers to test various signal detection and diversity schemes. Despite this progress at the macro-scale, there remains no viable pathway to downscale the testbeds to the nano-scale (Fig. 6.4).

6.3.1.1 Challenges with Wireless Energy Efficiency

In the previous section, we reviewed the growing focus on increasing the energy efficiency of both mobile and fixed wireless systems. Whilst we have built up a good understanding of power consumption mechanisms in terrestrial mobile networks, we still lack understanding in how nano-machines can communicate in an energy efficient manner. As communications and energy is vital for coordination and control of any system, so too will they be for nano-machines. It is envisaged that nano-scale communications will be critical to nano-machines that seek to coordinate tasks such as in vivo drug delivery and surgery [31]. Whilst many meso- and macro-scale in vivo medical devices (i.e., pacemaker) are battery powered, nano-batteries (50 μm [36]) are still significantly larger or of the same dimension as

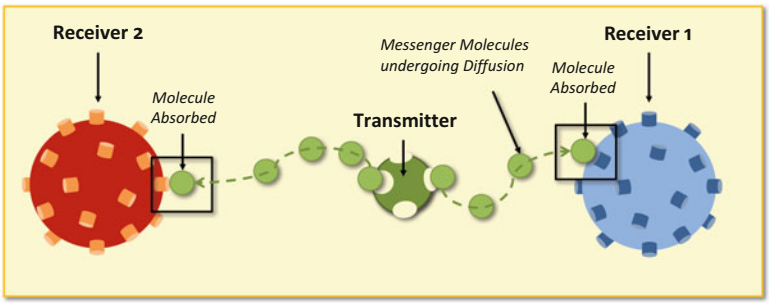

Fig. 6.4 Illustration of molecular communications via diffusion (MCvD) with a single emitter and multiple absorbing receivers

their nano-machine counter-parts. Therefore, charging batteries using externally generated acoustic [37] and electromagnetic radiation is not always viable and furthermore, nano-machines can be embedded in vivo areas that are either sensitive to radiation or difficult for radiation to penetrate. As such, energy harvesting from the nano-machines' locality is needed, i.e., the energy source should be near the nano-machine. Over the past decade, there is increasing interest to harvest energy from communication signals and achieve simultaneous wireless information and power transfer (SWIPT). In this chapter, we draw on our understanding of energy consumption and harvesting knowledge in current wireless systems to better understand nano-scale communications and exploit opportunities.

6.3.1.2 Challenges with Wave-Based Systems

The traditional practices of wireless planning with known coverage areas and propagation environments start to breakdown at the micro- and nano-scales. Communication systems in complex biological environments must be: bio-compatible, low-power consumption, low complexity, small dimension, and achieve reliable signaling in a fluid environment with complex cell/tissue obstacles. Such constraints are challenging for both EM-based THz systems and nano-acoustic systems. Current electricity and wave-based information delivery cannot downscale to the nano-scale whilst retaining the required level of propagation robustness and energy efficiency in vivo fluidic environments.

6.3.2 Molecular Communication via Diffusion

For centuries, scientists have known that molecular signaling underpins biological processes across multiple distance scales: from microscopic cell regulation to long range insect signaling. Inspired by the abundant use of molecules in biological signaling, Molecular communication via diffusion (MCvD) utilizes *molecular signal* (i.e., a chemical pulse) as an alternative carrier for information [33]. MCvD avoids the limitations of wave generation and propagation, and allows the signal to both persist and propagate to areas that are difficult to reach [38, 39]. The information in MCvD can be repetitive signaling from a limited alphabet, which is common in biological systems; or generic information from a rich alphabet, which is more common in human interaction. Historically, molecular-based signaling between animals has been observed since the ancient times, and more explicit arguments relating signaling success and natural selection were articulated by Darwin in 1871 [40]. It is only in the last decade or so that molecular communication from a telecommunications and information theory perspective has been explored [41]. Primarily, this has been due to the rise in demand from nano-scale engineering

(e.g., communication between swarms of nano-robots for targeted drug delivery [42]) and also the demand for industrial sensing in adverse environments. In both of these cases, the local environment can be adverse to the efficient propagation of electromagnetic (EM) wave signals.

Intense interest in molecular signaling between external bodies began over two decades ago, the scientific community paid particular interest to the pulse modulation techniques used by moths to attract mating partners [43]. Over the last decade, observations showed that chemical signals were encoded and decoded both in the time- and spatial-domains to assist homing and message delivery [44], and the moth's antenna system has been successfully reverse-engineered using biochemical sensors [45]. A more generalized communication system capable of transmitting any alpha-numeric message was later devised and built [34], linking the aforementioned bioengineering research with the field of telecommunication. In recent years, a growing body of significant molecular communication research has been devoted to a wide range of channel modeling [46] and telecommunication system design [47–49], information theory [50, 51], sensor and circuit design [45, 52], as well as biological system modeling [53, 54]. Furthermore, information theorists have become interested in the achievable reliable information rate of the random walk channel [50]. This led to various channel models been constructed, including and not limited to the capacity of a delay-time modulated channel [51].

With the advent of IoBNT systems in nano-medicine, there is an urgent need to connect various elements and sub-systems together to perform coordinated action. Yet, engineers simply do not know how to design and build nano-scale communication systems that can operate reliably and efficiently in vivo environments over long durations. Existing work in molecular communications has extended earlier understanding of chemical signals to transmit continuous information (i.e., a sequence of distinctive data packets, as opposed to repetitive data). As such, challenges in encoding and transmission strategies that relate to inter-packet chemical interference arise, which are exasperated by the stochastic nature of molecular diffusion channels.

6.3.3 Biological Communication and Energy Harvesting Systems

In biology, chemical signaling using molecules exchanges information and energy. In this subsection, we review some of the chemical signaling mechanisms in the communications context. In particular, we focus on biological cell signaling, which is essential to organized behaviour in multi-cellular organisms. A human body contains 100 trillion cells that coordinate actions through chemical signaling. Whilst the distances in cell signaling are typically small, hormone signals can transverse over long distances (i.e., several metres in the blood stream). A mixture of reception models exist. For example, signal receptors exist both within the cell

cytoplasm and on the surface of the cell membrane. Cell surface receptors often use secondary messengers to transmit an amplified signal to the cytoplasm. Adjacent cells often form direct passages that link their cytoplasms, permitting the passage of messengers.

6.3.3.1 Intra- and Inter-Cell Signaling

A variety of chemical macromolecules are used for signaling, including but not limited to peptides, proteins, dissolved gases, amino acids, nucleotides, steroids, and other lipids. Cell receptors are designed only to react to certain chemical signals, whilst ignoring the large volume and diversity of other signals. Receptor proteins have unique shapes that fit the shape of a specific signal molecule. Binding with the right signal will produce a response within the cell. *Intra-cell* signaling only affects a single cell and is divided into two categories. Intracrine occurs within the cell, binding to receptors inside the cell's cytoplasm and is used to regulate intracellular events. Autocrine signaling also affects the host cell, but the chemical messenger is ejected out of the cell and binds to the surface receptors of the cell. *Inter-cell* signaling affects a secondary cell or cells. Inter-cell signaling occurs across multiple distance scales, from a few microns (adjacent cells), to a metre (across the human body). Juxtacrine signaling is a contact dependent signaling process that allows chemical messengers to transverse via a ligand, junction, or matrix to another attached cell (see Fig. 6.5a). Longer distance cell-to-cell communications is called paracrine signaling. Here, cells eject molecular messengers that diffuse to a local cell, a few hundred microns away (see Fig. 6.5b). Longer distance diffusion communications occurs across the body between gland cells. This is known as endocrine signaling. The gland cells excrete hormones that use the circulatory system to be carried to target organ cells (see Fig. 6.5c).

The diffusive nature of endocrine signaling means that distant communications is slow. The nervous system provides rapid communication between distant cells and this is called *synaptic signaling*. Fiber extensions of nerve cells release neurotransmitters (chemical messengers) from their tips close to the target cells via the synaptic gap (see Fig. 6.5d). In addition to the aforementioned four techniques, some signals perform autocrine signaling, where it secrets signals for the sole purpose of binding to its own receptors, reinforcing developmental changes.

6.3.3.2 GABA Re-Uptake Mechanism

Energy harvesting using signaling molecules is common in biology at the cellular level. One such biological example that utilizes two types of molecules is the GABA re-uptake mechanism at the synaptic cleft. Glial cell absorbs/harvests GABA molecules and converts them to glutamine for utilizing at the signaling mechanisms

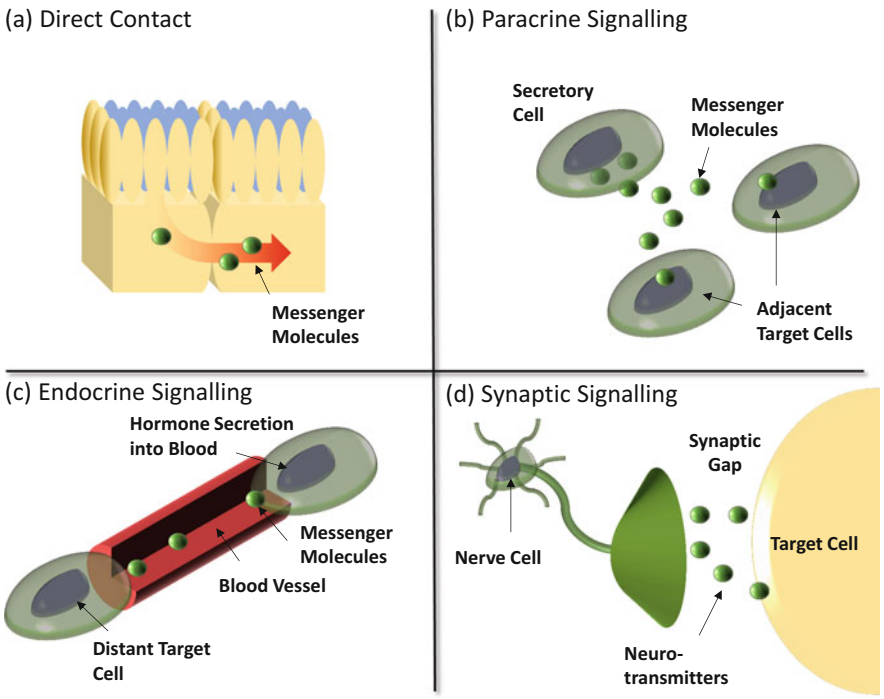

Fig. 6.5 Four kinds of cell signaling: (**a**) Juxtacrine signaling—cells in direct contact with each other send signals across junctions. (**b**) Paracrine signaling—secretions from one cell have an effect only on cells in the immediate area. (**c**) Endocrine signaling—hormones are released into the circulatory system, which carries them to the target cells. (**d**) Synaptic signaling—transmission of signal molecules (neurotransmitters) from a neuron over a small synaptic gap to the target cell

of presynaptic region. Type A molecule generated by the source is absorbed and converted to type B molecule inside the receiving node to be utilized in another subsequent signaling mechanism. The γ-Aminobutyric acid (GABA) metabolism and uptake is widely distributed across almost all regions of mammalian brain. GABA is constructed by glutamate via enzymatic reaction with glutamic acid decarboxylase (GAD) in the presynaptic neuron cell, which is then released as a neurotransmitter for sending signal to both neighbour Glia cells and postsynaptic neuron cells via GABA transporters (GATs). In this example, the presynaptic neuron cell acts as the source to emit the GABA as type A molecule, and Glia cell acts as the molecule harvesting node, and emit glutamine as type B molecule in response to the electrical charge polarization caused by GABA. This example of molecular signaling and simultaneous molecule harvesting demonstrates the dual usage of signaling molecules in biology.

6.3.4 Nano-Scale Energy Models

Almost all nano-scale systems have biological equivalents, which lends us an opportunity to better understand the energy levels involved. Biochemical processes in a cell are performed by molecular machines (mostly protein based). Molecular machine building blocks are constructed from single to multiple molecules. These building blocks are generally divided between passive mechanisms (i.e., switches react to a chemical stimulant) and active mechanisms (i.e., actuators consume energy to perform an action) [55]. Unlike macroscopic machines, molecular machines operate at energy scales close to the thermal energy, i.e., kT, where k is Boltzmann's constant and T is the temperature. Many of the motor actions are driven by non-equilibrium thermodynamics, converting force (i.e., chemical potential) into flux (motor movement, chemical flow). This process is known as free energy transduction. There are many examples of molecular motors in action, such as the muscle myosin, which is a motor that causes muscle contraction by converting ATP (chemical fuel) into mechanical work (i.e., for ATP hydrolysis the energy is $20kT \approx 4$ zJ).

6.3.5 Nano-Scale Propagation Models

The power expenditure model of a generic wireless system can be approximately modularized into a number of contributing components. In this paper, the authors focus on the propagation layer of consumption (including the data modulation, amplification, antenna loss, and propagation effects). The overhead consumption due to signal processing and cooling elements are left for future discussions. The main factors are: (1) the receiver antenna gain with radius R, (2) the free-space propagation loss λ, (3) the transmitter efficiency (i.e., power amplifier efficiency μ or chemical synthesis cost ϕ), (4) absorption loss τ (also known as transmittance), and the (5) the circuit power consumption. In general, the received electromagnetic (EM) power (P_{Rx}) or molecular number (N_{Rx}) is a small fraction of the total power extracted by the transmitter P_{Total}:

$$\begin{aligned} \frac{P_{\text{Rx}}}{P_{\text{Total}}} &\propto \mu \times \tau \left(\frac{R^2}{d^{\alpha}} \right) \quad \text{for EM} \\ \frac{N_{\text{Rx}}}{P_{\text{Total}}} &\propto \frac{1}{\phi (n_{\text{Tx}} - 1)} \times \left(\frac{R}{d + R} \right) \quad \text{for MCvD: } t \to \infty, \end{aligned} \tag{6.4}$$

assuming that the communication circuit power is relatively small in a nano-machine. Like RF communications, there is an energy efficiency factor for generating N_{Tx} molecules for transmission. This is related to the number of basic chemical

components per molecule n_{Tx} and the energy cost to bind or synthesize them ϕ [56, 57]. We now explain the reasoning and details of the efficiency equations given in Eq. (6.4) in the rest of the section.

6.3.5.1 THz Electromagnetic (EM) Communications

We first examine the EM communications case. One can see that the best achievable efficiency in Eq. (6.4) is limited by $d^{-\alpha}$ for EM and limited by $\tau d^{-\alpha}$ for THz nano-scale communications (where $\tau \propto \exp(-kfd)$). The absorption loss τ is log-linear proportional to absorption coefficient k, which depends on the chemical composition of the medium and is typically 1×10^{-5} for air and $1-3$ for water at $f = 0-10$ THz [58]. To illustrate the aforementioned reasoning, we show an illustration of radio wave versus molecular propagation in Fig. 6.6. In the (a) subplot, an isotropic EM

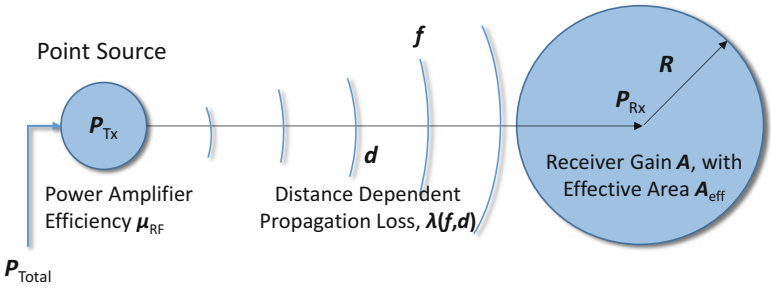

(a) Radio Frequency (RF) Channel

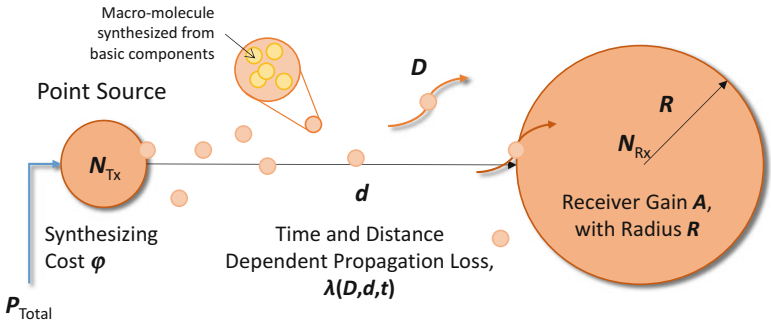

(b) Molecular Communication via Diffusion (MCvD) Channel

Fig. 6.6 Illustration of power loss in transmitting signals in (**a**) electromagnetic (EM) wave communications, and (**b**) Molecular communications via diffusion (MCvD)

antenna transmits to a receiver antenna with an effective area $A_{\text{eff}} \propto (fR)^2$, and the resulting received power after propagating a distance of d is $\mu_{\text{EM}} \frac{R^2}{d^{-\alpha}}$, where the value of μ_{EM} is typically 10–30% for EM systems [59].

6.3.5.2 Molecular Communication via Diffusion

MCvD, on the other hand, relies on message bearing molecules to freely diffuse from the transmitter to the receiver. We do not consider the base energy cost of physical matter (i.e., the molecules) as matter is not lost in the communication process. We do consider the energy cost of creating specific chemical compounds, as well as the energy benefits of restructuring the compound. In general, MCvD involves messenger molecules performing a random walk motion across the communication channel through collision interaction and a diffusion gradient. For each emitted molecule, there is a finite probability that it will reach the intended receiver. The power in the system at any given time instance is proportional to the number of molecules. Whilst the stochastic process is intuitively unreliable and requires a transmission time that is orders of magnitude longer than wave propagation, these deficiencies can be mitigated by communicating at very small distances (microns) or with the aid of strong ambient flow. For a basic random walk process, consider (as in Fig. 6.6b) a point emitter that transmits N_{Tx} molecules. The full absorption receiver, will capture N_{Rx} molecules given by Yilmaz [46]:

$$N_{\text{Rx}} = N_{\text{Tx}} h_c, \quad h_c = \left(\frac{R}{d+R}\right) \frac{d}{\sqrt{4\pi D t^3}} e^{\frac{-d^2}{4Dt}}, \tag{6.5}$$

where h_c is known as the *first passage time* density distribution.

The resulting expected number of received molecules up to time $t = T$ is $N_{\text{Tx}} F_c$, where $F_c = \frac{R}{d+R} \text{erfc}(\frac{d}{\sqrt{4DT}})$. This converges to N_{Tx} for 1-dimensional (1-D) space and $N_{\text{Tx}} \frac{R}{d+R}$ for 3-D space as $t \to \infty$ [60]. This means the full harvest of all transmitted molecules is possible in certain conditions, independent of the transmission distance. Naturally, the reality is that molecules will have a half life and not all data bearing molecules can be harvested. Reactions with other chemicals (i.e., enzymes) in the environment can reduce the effectiveness of energy harvesting in MCvD over time [61]. Yet, the potential to capture the vast majority of the transmitted molecules due to the random walk nature of propagation demonstrates the potential of MCvD over wave-based transmission. As with EM communications, there is a cost to produce the N_{Tx} molecules at the source in the first place. This can be shown to be [57]: $P_{\text{Total}} = \phi(n_{\text{Tx}} - 1)N_{\text{Tx}}$, where ϕ is the synthesizing cost of bonding n_{Tx} amino acids per transmitted molecule.

Comparing MCvD with EM propagation at the macro-scale to draw similar levels of performance (see Fig. 6.7), the received EM power is $\propto d^{-\alpha}$, where α typically varies between 2 and 4. On the other hand, the received molecules from MCvD can asymptotically be $\propto d^{-1}$, and at best independent of d in 1-D space, provided

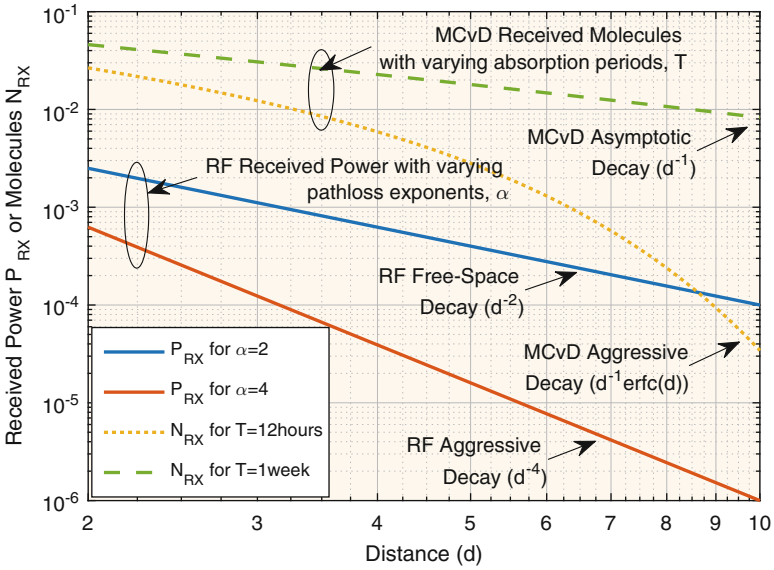

Fig. 6.7 Plot of received EM power (P_{Rx}) or MCvD molecules (N_{Rx}) for different transmission distances (d). The results show that MCvD can achieve asymptotic distance-dependent power decay at the rate of $\propto d^{-1}$, which is superior to all EM scenarios. Modeling parameters: mass diffusivity (water molecules in air) $D = 0.28\,\mathrm{cm}^2/\mathrm{s}$, EM frequency 5 GHz with parabolic receiver antenna $A_{\mathrm{eff}} = 0.56\,\pi\mathrm{R}^2$, and receiver radius of $R = 10\,\mathrm{cm}$

the receiver is willing to wait for a long time $t \to \infty$. Yet, the long waiting time is not as ridiculous as it may appear for the following two reasons. Firstly, the rate of diffusion is in reality accelerated by ambient air flow (i.e., convection currents) or shortened to a few milliseconds at the nano-scale. Secondly, when one transmits a continuous stream of symbols, the power emitted for the first symbol will be recovered by the N-th symbol's time (when N is large). Hence, there are no incurred delays to power or energy recovery in MCvD, provided a long stream of information symbols are transmitted (Fig. 6.8).

Several aspects of the previously reviewed biological processes can inspire engineers to design energy efficient communication systems at the nano-scale. As mentioned previously, the GABA is constructed by glutamate via enzymatic reaction with glutamic acid decarboxylase (GAD) in the presynaptic neuron cell, which is then released as a neurotransmitter for sending signal to both neighbour Glia cells and postsynaptic neuron cells via GABA transporters (GATs). In this example, the presynaptic neuron cell acts as the source to emit the GABA as type A molecule, and Glia cell acts as the relay, and emit glutamine as type B molecule in response to the electrical charge polarization caused by GABA. Note that the energy harvesting relay can also be engineered in cell by using genetic circuits with chemical reaction promoted by certain catalyst. The idea of using biological circuits for engineering transmitter and receiver in molecular communication system has already been studied.

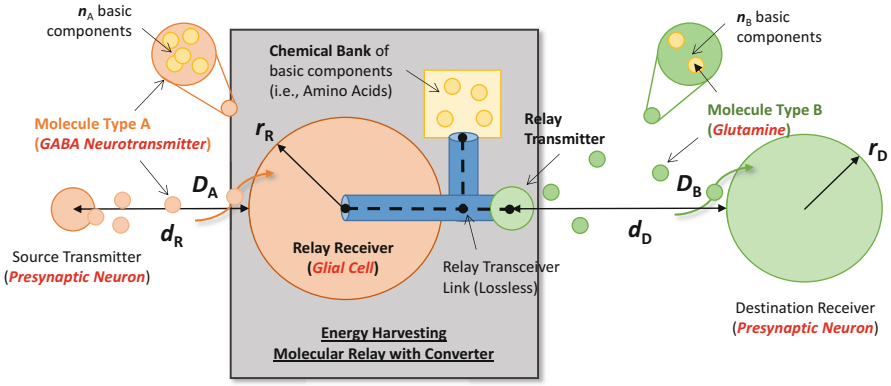

Fig. 6.8 Illustration of molecular relay communications with simultaneous energy harvesting. The mechanism is similar to the GABA biological mechanism in recycling molecules and converting molecular types through fragmentation and synthesis

6.3.6 *Molecular Crowd Harvesting*

As shown previously, despite the growing density of RF transmissions across multiple spectrum bands, the amount of energy available to harvest is dominated by the closest high power link. The rapid loss in RF energy due to transmission distance limits the potential for crowd harvesting, and unless all the transmitters are spaced equal distant to the receiver, crowd harvesting energy from N transmitters is not significantly superior to receiving energy from the nearest transmitter. For MCvD systems, as mentioned in Sect. 6.2, the energy of molecules does not obey the propagation laws of waves. Instead of experiencing a hostile $\propto d^{-\alpha}$ rate of energy decay, molecular numbers (or energy) decay $\propto d^{-1}$. Therefore, the potential to harvest energy from a field of transmitters is far greater for MCvD than for RF communications. If one assumes that the molecular transmitters are randomly and uniformly distributed according to a Poisson Point Process (PPP) or Poisson Cluster Process (PCP), one can leverage on existing stochastic geometry techniques [62] to find the expected molecular energy. This typically involves understanding the general distance distribution $f_D(d, n)$ from the energy harvesting node to the n-th nearest transmitter node [63].

Figure 6.9 shows a simulation of crowd harvesting energy from a formation of nodes distributed according to a modified Thomas PCP. Subplot (a) shows an instant snap-shot of the PCP formation of nodes with an energy harvesting receiver at the centre. Subplot (b) shows a scatter and box plot of the percentage of energy harvested for MCvD and RF transmissions. The results show that RF energy harvesting is far more sensitive to the density of transmitter nodes than MCvD energy harvesting. The random walk nature of molecular propagation means that the distance distribution (i.e., $f_D(d, n)$) is not a key consideration in crowd harvesting, whereas it is for RF systems. This demonstrates the potential for crowd harvesting in

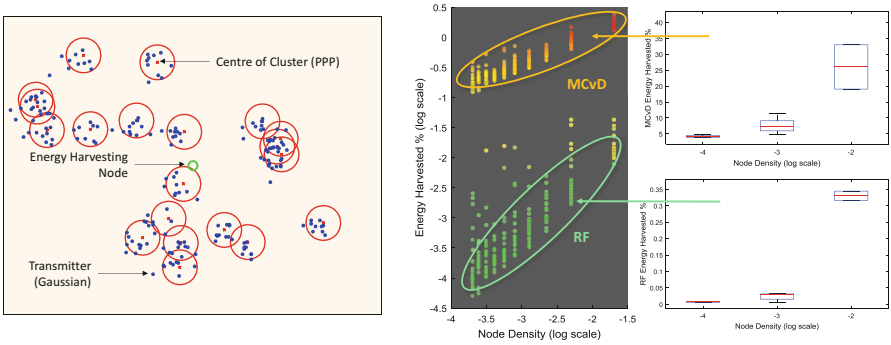

(a) Transmitters Distributed in a Modified Thomas PCP

(b) Scatter and Box Plot of Energy Harvested for Node Densities

Fig. 6.9 Crowd harvesting energy from a formation of nodes distributed according to a Thomas PCP. Subplot (**a**) shows an instant snap-shot of the PCP formation of nodes with an energy harvesting receiver at the centre. Subplot (**b**) shows a scatter and box plot of the percentage of energy harvested for MCvD and RF transmissions as a function of node density (per m^2). Modeling parameters: a variable modeling area radius 0.1–1 km, 20 clusters each with 10 nodes 2D Gaussian distributed with s.d. 30 m, mass diffusivity $D = 79.5\,\mu m^2/s$, pathloss exponent $\alpha = 2$, transmit power $P_{Tx} = 1$ W, transmit molecule $N_{Tx} = 1$, and receiver radius of $R = 1$ m

molecular systems, which can achieve 2–5 dB improvement in harvesting efficiency compared to RF systems in a similar setting, with the highest relative gain at low node densities.

6.4 Conclusions and Future Work

The performance of communication systems is fundamentally limited by the loss of energy through propagation and circuit inefficiencies. In this chapter, we have shown that it is possible to achieve ultra-low energy communications across different device size and transmission distance scales.

At the macro-scale, we have reviewed recent progress in simultaneous energy and information transfer for large-scale networks. It can greatly reduce the use of battery power and increase the availability and reliability for relaying. Through a case study, we show that it is better to harvest energy from TV bands in LoS channels and ambient Wi-Fi signals in NLoS conditions. Furthermore, we have discussed the optimization of transmissions in crowd harvesting, especially with the use of node collaboration.

At the nano-scale, we show that while the energy of waves will inevitably decay as a function of transmission distance and time, the energy in molecules does not. In fact, over time, the molecular receiver has an opportunity to recover some, if not all of the molecular energy transmitted. Inspired by the GABA metabolism system in nature, which fragments and reassembles molecules, we discuss a number of communication systems. For point-to-point links, we found that given sufficient time, the energy harvested can be fully recovered in 1-D channels and scales with

d^{-1} in 3-D channels. This fundamentally improves over wave-systems that have a free-space upper-bound of d^{-2}. For more complex systems, we designed two relay systems that can achieve high energy harvesting efficiency (12–25% at the relay). For parallel channels, we found that molecular communications offer superior energy harvesting scaling with node density (2–5 dB gain) and are significantly less sensitive to the spatial distribution of nodes. Regarding the information capacity, the generalized capacity remains to be discovered, but capacity limits for specific modulation schemes exist and are beyond the scope of this paper. In summary, chemically manipulation to improve energy efficiency of information transmission is something that has no parallel in radio frequency communications. What currently remains beyond engineering capabilities is the ability to build such biological functionalists into realistic systems. Nonetheless, the preliminary results in this article indicate that the potential for simultaneous molecular information and energy transfer (SMIET) is immense and further cross-discipline research is needed to transform theory to reality.

References

1. S. Bi, C. Ho, R. Zhang, Wireless powered communication: opportunities and challenges. IEEE Commun. Mag. **53**(4), 117–125 (2015)
2. M. Pinuela, P. Mitcheson, S. Lucyszyn, Ambient RF energy harvesting in urban and semi urban environments. IEEE Trans. Microwave Theory Tech. **61**(7), 2715–2726 (2013)
3. F. Iannello, O. Simeone, U. Spagnolini, Medium access control protocols for wireless sensor networks with energy harvesting. IEEE J. Sel. Areas Commun. **60**(5), 1381–1389 (2012)
4. W. Brown, The history of power transmission by radio waves. IEEE Trans. Microwave Theory Tech. **32**, 1230–1242 (1984)
5. B. Han, R. Nielsen, C. Papadias, R. Prasad, Radio frequency energy harvesting for long lifetime wireless sensor networks, in *International Symposium on Wireless Personal Multimedia Communications* (2013), pp. 1–5
6. T. Ajmal, D. Jazani, B. Allen, Design of a compact RF energy harvester for wireless sensor networks, in *IEEE Conference on Wireless Sensor Systems*, June (2012), pp. 1–5
7. T. Ajmal, V. Dyo, B. Allen, D. Jazani, I. Ivanov, Design and optimisation of compact RF energy harvesting device for smart applications. Electron. Lett. **50**(2), 111–113 (2014)
8. S. Lee, R. Zhang, K. Huang, Opportunistic wireless energy harvesting in cognitive radio networks. IEEE Trans. Wirel. Commun. **12**, 4788–4799, (2013)
9. W. Guo, S. Wang, Mobile crowd-sensing wireless activity with measured interference power. IEEE Wirel. Commun. Lett. **2**, 539–542 (2013)
10. I. Krikidis, Simultaneous information and energy transfer in large-scale networks with/without relaying. IEEE Trans. Commun. **62**, 900–912 (2014)
11. W. Guo, S. Zhou, Y. Chen, S. Wang, X. Chu, Z. Niu, Simultaneous information and energy flow for IoT relay systems with crowd harvesting. IEEE Commun. Mag. **54**(11), 143–149 (2016)
12. EARTH, WP2.D2.3: energy efficiency analysis of the reference systems. Energy Aware Radio and Network Technologies (EARTH), Technical Report, December (2010)
13. S. Zaidi, A. Afzal, M. Hafeez, D. McLernon, M. Ghogho, Solar energy empowered cognitive metro cellular networks. IEEE Commun. Mag. **53**(7), 70–77 (2015)
14. O. Ozel, K. Shahzad, S. Ulukus, Optimal energy allocation for energy harvesting transmitters with hybrid energy storage and processing cost. IEEE Trans. Signal Process. **62**(12), 3232–3245 (2014)

15. J. Fakidis, S. Videv, S. Kucera, H. Claussen, H. Haas, Indoor optical wireless power transfer to small cells at nighttime. IEEE J. Lightwave Technol. **34**(13), 3236–3258 (2016)
16. O. Ozel, K. Tutuncuoglu, J. Yang, S. Ulukus, A. Yenner, Transmission with energy harvesting nodes in fading wireless channels: optimal policies. IEEE J. Sel. Areas Commun. **29**(8), 1732–1743 (2011)
17. T. Le, K. Mayaram, T. Fiez, Efficient far-field radio frequency energy harvesting for passively powered sensor networks. IEEE J. Solid-State Circuits **43**(5), 1287–1302 (2008)
18. D. Pavone, A. Buonanno, M. D'Urso, F.G.D. Corte, Design considerations for radio frequency energy harvesting devices. Prog. Electromagn. Res. B **45**, 19–35 (2012)
19. E. Nan, X. Chu, W. Guo, J. Zhang, User data traffic analysis for 3G cellular networks, in *IEEE International ICST Conference on Communications and Networking in China*, August (2013), pp. 468–472
20. U. Olgun, C. Chen, J.L. Volakis, Investigation of rectenna array configurations for enhanced RF power harvesting. IEEE Antennas Wirel. Propag. Lett. **10**, 262–265 (2011)
21. M. Haenggi, *Stochastic Geometry for Wireless Networks* (Cambridge University Press, Cambridge, 2012)
22. S. Wang, W. Guo, M. McDonnell, Distance distributions for real cellular networks, in *IEEE Conference on Computer Communications (INFOCOM)* (2014), pp. 181–182
23. M. Haenggi, On distances in uniformly random networks. IEEE Trans. Inf. Theory **51**, 3584–3586 (2005)
24. R. Ganti, M. Haenggi, Interference and outage in clustered wireless ad hoc networks. IEEE Trans. Inf. Theory **55**(9), 4067–4086 (2009)
25. S. Kumar, E. Hamed, D. Katabi, L.E. Li, LTE radio analytics made easy and accessible, in *ACM Special Interest Group on Data Communication (SIGCOMM)*, August (2014), pp. 1–12
26. I. Pocsik, Lognormal distribution as the natural statistics of cluster systems. Eur. Phys. J. D At. Mol. Opt. Plasma Phys. **20**(1), 395–397 (1991)
27. M. Laner, P. Svoboda, S. Schwarz, M. Rupp, Users in cells: a data traffic analysis, in *IEEE Wireless Communications and Networking Conference (WCNC)*, April (2012), pp. 3063–3068
28. W. Guo, S. Wang, Radio-frequency energy harvesting potential: a stochastic analysis. Trans. Emerg. Telecommun. Technol. **24**, 453–457 (2013)
29. 3GPP, TR36.814 V9.0.0: further advancements for E-UTRA physical layer aspects (Release 9), 3GPP. Technical Report, March (2010)
30. D. Lee, S. Zhou, X. Zhong, Z. Niu, X. Zhou, H. Zhang, Spatial modeling of the traffic density in cellular networks. IEEE Wirel. Commun. **21**(1), 80–88 (2014)
31. I.F. Akyildiz, M. Pierobon, S. Balasubramaniam, Y. Koucheryavy, The internet of bio-nano things. IEEE Commun. Mag. **53**(3), 32–40 (2015)
32. D. Piraner, M. Abedi, B. Moser, A. Lee-Gosselin, M. Shapiro, Tunable thermal bioswitches for in vivo control of microbial therapeutics. Nat. Chem. Biol. **13**(1), 75–80 (2016)
33. N. Farsad, H. B. Yilmaz, A. Eckford, C.-B. Chae, W. Guo, A comprehensive survey of recent advancements in molecular communication. IEEE Commun. Surv. Tutorials **18**(3), 1887–1919 (2016)
34. N. Farsad, W. Guo, A. Eckford, Tabletop molecular communication: text messages through chemical signals. PLoS ONE **8**, e82935 (2013)
35. B. Koo, C. Lee, H. Yilmaz, N. Farsad, A. Eckford, C. Chae, Molecular MIMO: from theory to prototype. IEEE J. Sel. Areas Commun. **34**(3), 600–614 (2016)
36. S. Gowda, A. Reddy, X. Zhan, P. Ajayan, Building energy storage device on a single nanowire. ACS Nano Lett. **11**(8), 3329–3333 (2011)
37. M. Donohoe, S. Balasubramaniam, B. Jennings, J.M. Jornet, Powering in-body nanosensors with ultrasounds. IEEE Trans. Nanotechnol. **15**(2), 151–154 (2016)
38. S. Qiu, W. Guo, S. Wang, N. Farsad, A. Eckford, A molecular communication link for monitoring in confined environments, in *IEEE International Conference on Communications (ICC) - Workshops*, June (2014), pp. 718–723
39. W. Guo, C. Mias, N. Farsad, J.L. Wu, Molecular versus electromagnetic wave propagation loss in macro-scale environments. IEEE Trans. Mol. Biol. Multiscale Commun. (T-MBMC) **1**(1), 18–25 (2015)

40. T.D. Wyatt, Fifty years of pheromones. Nature **457**, 262–263 (2009)
41. T. Nakano, A. Eckford, T. Haraguchi, *Molecular Communication* (Cambridge University Press, Cambridge, 2013)
42. S. Chandrasekaran, D. Hougen, Swarm intelligence for cooperation of bio-nano robots using quorum sensing, in *IEEE Bio Micro and Nanosystems Conference*, January (2006), p. 141
43. A. Mafra-Neto R.T. Carde, Fine-scale structure of pheromone plumes modulates upwind orientation of flying moths. Nature **369**, 142–144 (1994)
44. P. Knusel, M. Carlsson, B. Hansson, T. Pearce, P. Verschure, Time and space are complementary encoding dimensions in the moth antennal lobe. Comput. Neural Syst. **18**, 35–62 (2007)
45. M. Cole, Z. Racz, J. Gardner, T. Pearce, A novel biomimetic infochemical communication technology: from insects to robots, in *IEEE Sensors* (2012), pp. 1–4
46. H.B. Yilmaz, A.C. Heren, T. Tugcu, C.-B. Chae, Three-dimensional channel characteristics for molecular communications with an absorbing receiver. IEEE Commun. Lett. **18**(6),929–930 (2014)
47. I.F. Akyildiz, F. Brunetti, C. Blazquez, Nanonetworks: a new communication paradigm. Elsevier Comput. Netw. **52**, 2260–2279 (2008)
48. I. Llatser, A. Cabellos-Aparicio, M. Pierobon, Detection techniques for diffusion-based molecular communication. IEEE J. Sel. Areas Commun. **31**(12), 726–734 (2013)
49. L. Felicetti, M. Femminella, G. Reali, T. Nakano, A.V. Vasilakos, TCP-like molecular communications. IEEE J. Sel. Areas Commun. **32**(12), 2354–2367 (2014)
50. B. Atakan, O. Akan, An information theoretical approach for molecular communication, in *IEEE Bionetics Conference*, December (2007), pp. 33–40
51. K. Srinivas, A. Eckford, R. Adve, Molecular communication in fluid media: the additive inverse Gaussian noise channel. IEEE Trans. Inf. Theory **8**, 4678–4692 (2012)
52. M. Pierobon, I.F. Akyildiz, A physical end-to-end model for molecular communication in nanonetworks. IEEE J. Sel. Areas Commun. **28**(4), 602–611 (2010)
53. S. Hiyama, Y. Moritani, T. Suda, R. Egashira, A. Enomoto, M. Moore, T. Nakano, Molecular communication, in *Technical Proceedings of the 2005 NSTI Nanotechnology Conference and Trade Show*, vol. 3 (2005), pp. 391–394
54. P. Lio, S. Balasubramaniam, Opportunistic routing through conjugation in bacteria communication nanonetwork. Elsevier Nano Commun. Netw. **3**, 36–45 (2012)
55. A. Coskun, M. Banaszak, R. Astumian, J. Stoddart, B. Grybowski, Great expectations: can artificial molecular machines deliver on their promise. Chem. Soc. Rev. **41**(1), 19–30 (2012)
56. T. Furubayashi, T. Nakano, A. Eckford, Y. Okaie, T. Yomo, Packet fragmentation and reassembly in molecular communication. IEEE Trans. Nanobiosci. **15**, 284–288 (2016)
57. M.S. Kuran, H.B. Yilmaz, T. Tugcu, B.O. Edis, Energy model for communication via diffusion in nanonetworks. Nano Commun. Netw. **1**(2), 86–95 (2010)
58. J. Jornet, I. Akyildiz, Channel modeling and capacity analysis for electromagnetic wireless nanonetworks in the terahertz band. IEEE Trans. Wirel. Commun. **10**(10), 3211–3221 (2011)
59. G. Auer, V. Giannini, C. Desset, I. Godor, P. Skillermark, M. Olsson, M. Imran, D. Sabella, M. Gonzalez, O. Blume, A. Fehske, How much energy is needed to run a wireless network? IEEE Commun. Mag. **18**(5), 40–49 (2011)
60. Y. Deng, W. Guo, A. Noel, M. Elkashlan, A. Nallanathan, Enabling energy efficient molecular communication via molecule energy transfer. IEEE Commun. Lett. **21**(2), 254–257 (2016)
61. A. Noel, K.C. Cheung, R. Schober, Improving receiver performance of diffusive molecular communication with enzymes. IEEE Trans. NanoBiosci. **13**(1), 31–43 (2014)
62. S. Akbar, Y. Deng, A. Nallanathan, M. Elkashlan, Downlink and uplink transmission in K-tier heterogeneous cellular network with simultaneous wireless information and power transfer, in *IEEE Global Communications Conference (GLOBECOM)*, 2015
63. W. Guo, Y. Deng, H.B. Yilmaz, N. Farsad, M. Elkashlan, C.-B. Chae, A. Eckford, A. Nallanathan, SMIET: simultaneous molecular information and energy transfer. IEEE Wirel. Commun. (2017, to appear)